

Investigation on High Performance of Graphite-Ionic Liquid Paste Electrode: Characterization and New Hypothesis

Xuzhi Zhang¹, Meng Li², Yi Cui¹, Jianxin Zhu¹, Jun Zhao¹, Bijuan Chen¹, Keming Qu^{1,*}

¹Yellow Sea Fisheries Research Institute, Chinese Academy of Fishery Sciences, Qingdao 266071, China

²School of Life Science and Technology, Dalian Ocean University, Dalian 116023, China

*E-mail: kmqu@ysfri.ac.cn

Received: 2 February 2013 / Accepted: 27 February 2013 / Published: 1 April 2013

We report on a graphite-based carbon paste electrode with the ionic liquid n-octylpyridinium hexafluorophosphate as the binder, and its characterization by electrochemical and optical techniques. Voltammetric studies reveal that the electrode has attractive features compared to conventional electrodes using paraffin, notably an improved sensitivity and an increased electron transfer rate. Distinct flakes have been identified on the electrode surface that possess sharp edges, randomly interlace together, and appear like mono- and/or multilayer graphene. The attractive electrochemical properties are presumed to result from the presence of mono- and/or multilayer graphenes that are formed during the grinding process and combine with the ionic liquid before they can aggregate as in case of exfoliated flakes. This kind of graphene with its edge plane characteristics provides a particularly high density of electrochemically active sites on the surface of the electrode.

Keywords: Ionic liquid; Graphene; Carbon paste electrode; Electrochemical performance; Mechanism

1. INTRODUCTION

The ability of ionic liquids (ILs) to promote the electrochemical performance of electrodes has been documented in connection with many important analytes [1]. Recently, they have been proposed to be very interesting and efficient pasting binders in place of non conductive organic binders for the preparation of carbon paste electrodes (CPEs) [1, 2] owing to their unique feature of good redox-robustness. It was demonstrated clearly that it would be advantageous to use ILs to fabricate CPEs due to their thermal stability and high conductivity.

Maleki et al. [3] found that one of the ILs-based CPEs allowed sensitive, low-potential, simple, low-cost, and stable electrochemical sensing of biomolecules and other electroactive compounds. Liu

et al. [4] reported that the CPE constructing with an imidazolium-based ionic liquid had increased the sensitivity of the response toward potassium ferricyanide. Sun et al. [5] also reported that ionic liquid-based CPEs were ideal basic platforms to fabricate biosensors. Compton et al. [6, 7] confirmed that IL-based CPEs showed very attractive electrochemical performances compared to other conventional electrodes using graphite and mineral oil, notably improved sensitivity and stability. The causation for the attractive electrochemical performance from the IL and graphite-based CPE (CILE) is interesting. However, there is not a clear conclusion until now.

In this paper, the electrochemical and electroanalytical properties of CILE, which was prepared using ionic liquid *n*-octylpyridinium hexafluorophosphate (OPFP, chemical structure shown in Fig. 1 inset) as a binder, were characterized by electrochemical methods in comparison with the traditional CPE made of paraffine and graphite powder (morphological features shown in Fig. 1). The attractive electrochemical and electroanalytical performances of the CILE were documented. And a new hypothesis on the formation of these performances was put forward and was test with the help of scanning electron microscopic and transmission electron microscopic techniques.

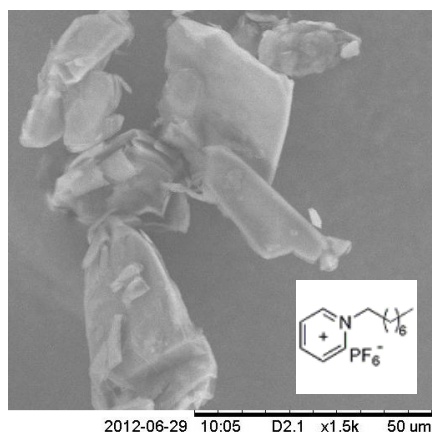


Figure 1. Image of graphite powder (Instruct name: TM-1000; Accelerating voltage: 1.5 kV; Emission current: 74500 nA). Inset: Chemical structure of *n*-octylpyridinium hexafluorophosphate (OPFP).

2. EXPERIMENTAL

2.1. Apparatus and chemical

Cyclic voltammetry (CV), differential pulse stripping voltammetric (DPSV), chronoamperometry and electrochemical impedance spectroscopy (EIS) were performed using a CHI 660D Electrochemical Analyzer (CH Instruments, Shanghai, China) with a three-electrode arrangement, consisting of a paste working electrode ($\Phi = 3.6$ mm), a saturated calomel reference electrode (SCE) and a platinum wire auxiliary electrode. Hitachi Tabletop Microscope TM-1000 was used to obtain the image of graphite powder. Scanning electron microscopic (SEM) measurements

were carried out on a JSM-6700F scanning electron microscope (Japan Electron Company). Transmission electron microscopic (TEM) micrographs were obtained using a JEM-1200EX transmission electron microscopy (JEOL, Japan).

Ionic liquid *n*-octylpyridinium hexafluorophosphate (OPFP) was purchased from Shanghai Chengjie Co., Ltd (Shanghai, China). Graphite powder (purity > 99.85; granularity: 30 μm ; surface area: 10-14 m^2/g) was made in Shanghai Colloid Chemical Plant (Shanghai, China). Calcein, diethylstilbestrol, and malachite green were purchased from Sigma (USA). The other usual reagents were purchased from Shanghai Chemical Reagent Co. (Shanghai, China) and were all of analytical reagent grade. Solutions were all prepared with sterilized ultrapure water (Resistivity: 18.2 $\text{M}\Omega\cdot\text{cm}$).

2.2. Fabrication of paste electrodes

One of the most important requirements for making a good CPE is stability. It has been documented that the electrode made from OPFP yielded a consistent composite with more favorable electrochemical characteristics [3, 6, 8, 9]. Thus OPFP was used as the ionic liquid binder to fabricate CILE. All paste electrodes were fabricated by conventional method described in previous reports [3, 6, 10] with minor modification. In brief, the required amount of OPFP was mixed using pestle and mortar with the needed amount of graphite powder for 30 min in room temperature, followed by being loaded into a glass tube (3.6 mm, i.d.). Then the glass tube was heat in an oven to a temperature higher than the melting point of OPFP (mp 65 $^{\circ}\text{C}$). The composite was packed tightly using a stainless stick. Electrical contact was established via a copper wire. It was then left to cool to room temperature. Although OPFP is a solid powder at room temperature, it has a sticky nature, so it tends to interact strongly with the graphite powder and forms a very mechanically stable solid composite upon mixing. The surface of this kind of CPE, which is abbreviated as CILE, can be polished very well and shows features similar to solid surfaces. Its surface was smoothed on a weighing paper and rinsed with pure water carefully prior to use. The CPE used as control was also fabricated by mixing paraffine and graphite powder with a ratio of 20/80 (w/w) [10].

2.3. Electrochemical measurements

Unless otherwise indicated, CV experiments were performed at a scan rate of 0.100 V/s; DPV experiments were performed at a pulse amplitude of 0.05 V, a pulse width of 0.05 s and a pulse period of 0.2 s. The EIS measurements were carried out in a 1.0 mmol/L $\text{K}_3[\text{Fe}(\text{CN})_6]$ solution containing 0.5 mol/L KCl. The AC voltage amplitude was 0.005 V and the voltage frequencies were ranged from 10 KHz to 0.1 Hz. The electrochemical analysis of Cd^{2+} included two steps: accumulation and stripping. Firstly, metallic cation was preconcentrated onto the electrode surface and then reduced to Cd^0 under -1.2 V (vs. SCE) for 120 s under stir. Secondly, reduced Cd^0 were oxidized to metallic cation during the anodic potential sweep. All experiments were conducted at room temperature (25 ± 0.5 $^{\circ}\text{C}$).

3. RESULTS AND DISCUSSION

3.1. Electrochemical area

According to previous reports [3, 10], a series of CILE s were prepared by mixing different percentages of graphite powder and OPFP to optimize the composition ratio. The outcome confirms that the ratio of 50/50 (w/w) is the most proper.

The electrochemical areas of the CILE and the CPE were evaluated using chronoamperometry in a 1.0 mM ferrocene monocarboxylic acid solution. The slope of the linear region of the $I-t^{-1/2}$ plot in the short time region provides the product $nFAC_0D^{1/2}\pi^{-1/2}$ using the Cottrell equation:

$$i_d = nFAC_0D^{1/2}(\pi t)^{-1/2} \quad (1)$$

where $C_0=1.0$ mM, $D=7.96 \times 10^{-10}$ cm²/s [11], are respectively, the concentration and diffusion coefficient of ferrocene monocarboxylic acid, and the other parameters have their usual meanings. Then, 0.169 cm² and 0.086 cm² were obtained for the electrochemical areas of the CILE and the CPE, respectively. The apparent geometric areas of the two kinds of paste electrodes are all 0.102 cm². As expected, the electrochemical area of the CPE exposed to the solution is smaller than the geometric area, with the remainder occupied by the insulating “host” [12]. However, the electrochemical area of the CILE is notable larger than its geometric area.

3.2. Electrochemical impedance spectroscopy characteristic

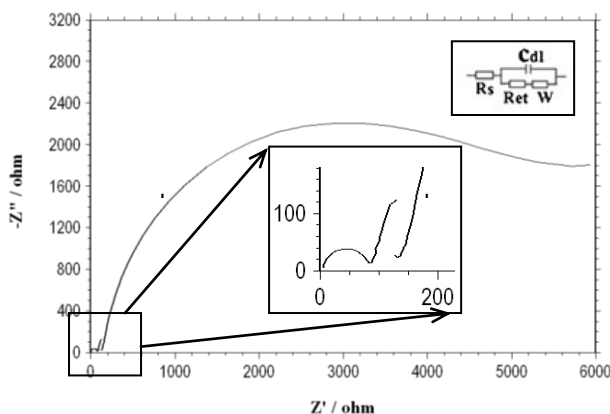


Figure 2. Electrochemical impedance spectroscopies of the CILE (a) and the CPE (b). Supporting electrolyte: 1.0 mM $K_3[Fe(CN)_6]$ solution containing 0.5 M KCl. Inset is the the Randles equivalent circuit.

Since the resistance for an electrode is one of the most important factors which affect electrochemical behavior, EIS measurement was employed to further investigate the CILE in comparison with CPE. Results show that serially connected charge transfer resistance (R_{ct}) for the

CILE is much smaller than that for the CPE (Fig. 2), indicating the IL-based electrode has faster charge transfer rate. The value of direct current resistance for the CILE is much smaller than that for the CPE, demonstrating higher charge transfer rate and electroactive area leading to high conductance [13].

3.3. Electroanalytical performances

Aiming to evaluate the electroanalytical performance of the CILE, a group of typical species, including potassium ferricyanide, methylene blue, diethylstilbestrol, calcein, malachite green and Cd^{2+} , were employed for measurements in comparison with the CPE.

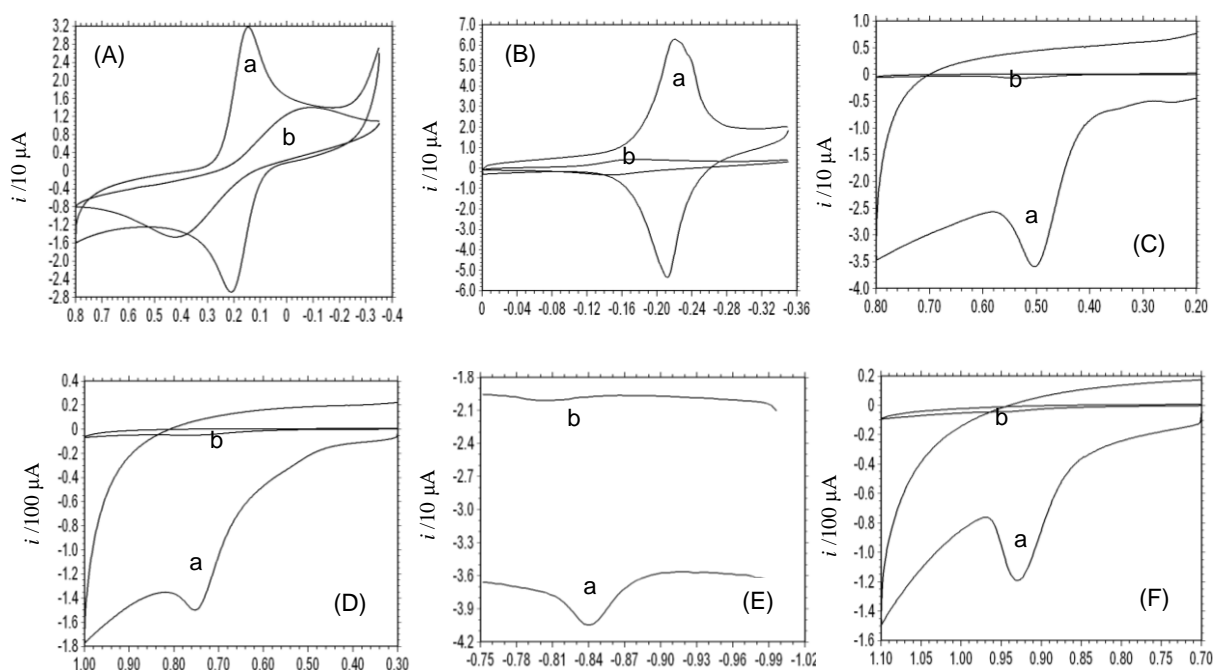


Figure 3. Voltammograms of 1.0 mmol/L potassium ferricyanide in 0.5 mol/L KCl solution (A), 50 $\mu\text{mol/L}$ methylene blue in phosphate buffer solution of pH 6.5 (B), 0.31 $\mu\text{mol/L}$ diethylstilbestrol in phosphate buffer solution of pH 6.5 (C), 3.2 $\mu\text{mol/L}$ calcein in phosphate buffer solution of pH 6.0 (D), 70 $\mu\text{mol/L}$ Cd^{2+} in phosphate buffer solution of pH 3.0 (E) and 20 $\mu\text{mol/L}$ malachite green in phosphate buffer solution of pH 6.5 (F) at the CILE (a) and CPE (b), respectively. Quit/accumulation times for potassium ferricyanide, methylene blue, diethylstilbestrol, calcein, and malachite green are 5 s, 60 s, 180 s, 240 s and 240 s, respectively. For the DPSV detection of Cd^{2+} : Accumulation at -1.2 V for 120 s with stir.

As shown in Fig. 3, at the CILE the current responses for all the species, both diffusion control reactions and adsorption control reactions, are higher significantly in comparison with that from the CPE, confirming the better collection ability and/or the larger electrochemical areas of the former electrode [3, 10]. For the reversible and the quasi-reversible species, for example, potassium

ferricyanide and MB, the differences between the anodic peak potential (E_{pa}) and the cathodic peak potential (E_{pc}), namely the ΔE_{ps} , are much smaller at the CILE than that at the CPE; for the irreversible species, the overpotential is lower obviously at the CILE than that at the CPE. These suggest that the CILE has strong catalytic activity. Certainly, the decrease of the overvoltage attributes to the large electrochemical area to some extent, owing to that the overpotential varies inversely with the current density. All contents mentioned above evidence that the CILE exhibits an excellent electroanalytical performance towards some species, which is in good agreement with previous reports [3, 8, 9].

3.4. Morphological characteristic

Herein we are very interested in the causation of the attractive electroanalytical performance of CILE. Since electrochemistry is based fundamentally on interfacial phenomena [10], the morphological features of the electrode surfaces were studied with high-magnification SEM method. Typically the CILE shows a uniform surface topography (Fig. 4), which is in good agreement with previous reports [3]. What's more, another especial feature attracted our attention: There are distinct flakes with very sharp edges on the surface of CILE, which randomly interlace together and are almost alike in the appearance of mono- or multilayer graphene [14, 15]. In fact, in some papers [8, 16] the feature can also be found clearly or faintly. However, no hypotheses have been put forward to explain the presence of the characteristic feature. It's the causation of the attractive electroanalytical performance? It's interesting that what happens during the process of the fabrication of the CILE

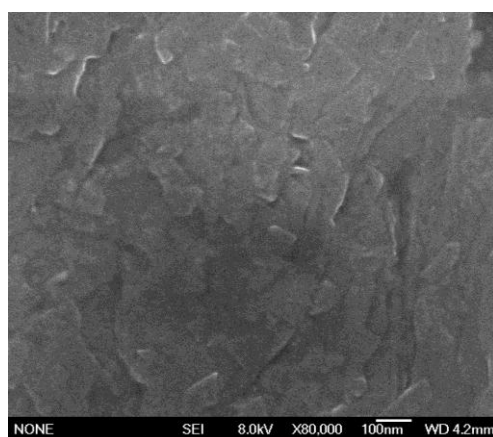
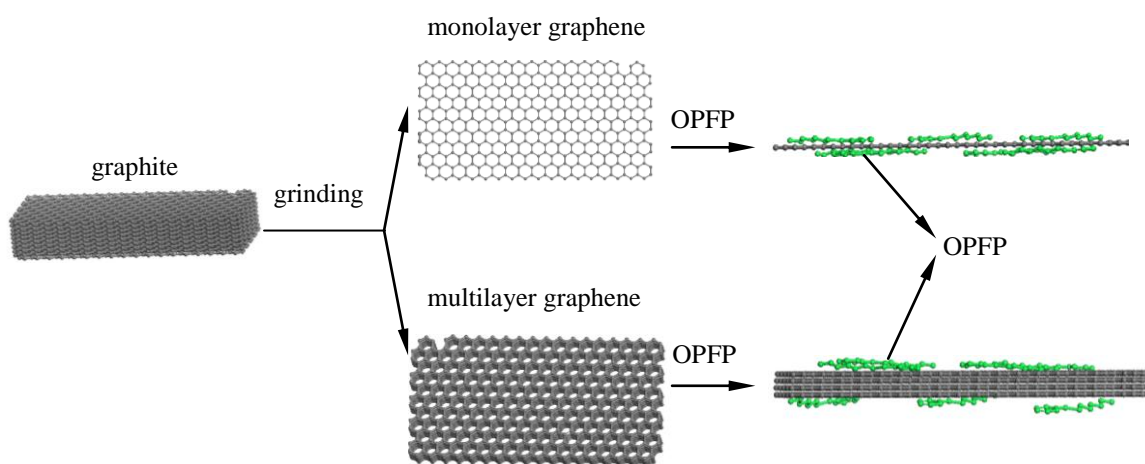


Figure 4. SEM image of the surface of CILE (Instruct name: JSM-6700F; Accelerating voltage: 8.0 kV).

3.5. New hypothesis

Since graphene layers stack one atop another and hold together in graphite only by weak van der Waals forces and π - π stacking [17], the shear forces can lead to a continuous delamination of ultrathin graphene flakes under mild grinding conditions [14, 18]. Let's try to understand them by hypothesizing that on the surface of the CILE there are graphene, which are produced during the

process of fabricating CILE. It has reported that the high exfoliation of graphite in IL is attributed to the surface tension of IL close to that of graphite, which favors the exfoliation process, and to the ionicity of IL, which stabilizes the exfoliated graphene sheets [19]. In other words, a combination occurs because the energy required to exfoliate graphene is balanced by the solvent-graphene interaction for solvents whose surface energy matches that of graphene [20]. Thus, the presence of ionic liquid OPFP helps to avoid agglomeration of the exfoliated flakes via interaction with the mono- or multilayer graphene by cation- π and/or π - π stacking [3], which balance the interaction between parallel layers. Consequently, stable mono- or multilayer graphene structures are formed (as shown in scheme 1).



Scheme 1. Schematic representation of the formation of graphene.

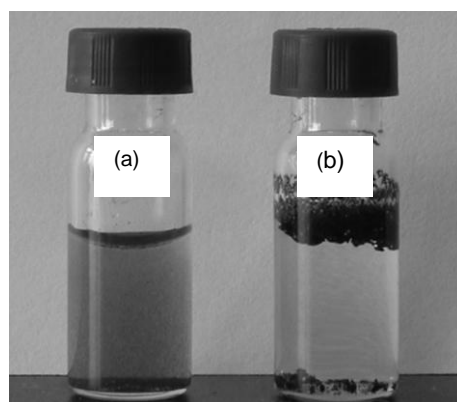


Figure 5. Photographs of vials containing 1 g/L graphite-OPFP composite (a) and 1 g/L graphite-paraffine composite (b) dispersed in water solution by ultrasonication. Photograph a was taken 35 min after the ultrasonication; photograph b taken 2 s after the ultrasonication.

To test the hypothesis put forward above, some physical experiments were carried out. As it is well known, graphite powder is insoluble in most solvents, especially in water. When the composite made by grinding paraffine and graphite powder was treated under ultrasonic in pure water for about 1 h, it keeps floating on the water phase (Fig. 5b). However, taking the place of paraffine by ionic liquid, OPFP, we can obtain a black and homogeneous suspension with numbers of macroscopic aggregates. After these aggregates were removed by mild centrifugation, the homogenous dark dispersion can remain for at least one week (Fig. 5a). Similar phenomena have been obtained when carbon nanotubes [21] and graphene were dispersed in water phase with the help of sodium dodecyl sulfate [22] or poly(diallyldimethylammonium chloride) [23], without impairing their other physical properties.

Further, the substances suspended in water phase were investigated with SEM and TEM methods. The typical images are shown in Fig. 6 and Fig. 7, respectively. In the SEM images, it's clear that there are mono- or/and multilayer graphene, which have the similar dimensions and structures as previous reports [14, 18, 19, 24, 25]. Majority of them show a knife-edge structure with a nanometer-sized-thick base and a 2–6 nanometer-thick sharp edge made of perfect graphitic layer. Thus we believe that, in these conditions, some of the graphite particles have been exfoliated to give mono- or multilayer graphene. The 2D dimensions of the flakes are a little larger than that obtained from the surface of the CILE. It's probably resulting from the treatment of polishing CILE prior test.

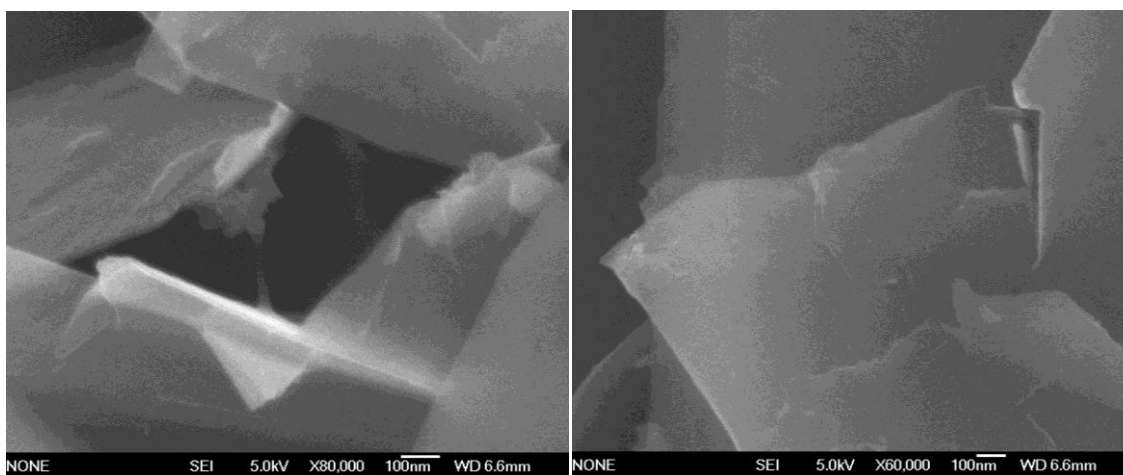


Figure 6. SEM images of 3D carbon/IL composite with high magnification (Instruct name: JSM-6700F; Accelerating voltage: 8.0 kV).

Fig. 7 shows the TEM images of carbon/OPFP composite obtained from the homogenous dark dispersion solution, also illustrating the flakelike shapes of graphene. Some regions appear just as that was reported previously [13, 22- 24]: There are some corrugations and scrollings on the edge of the graphene. This nature of corrugations and scrollings is highly beneficial in maintaining a high surface area on the electrode since the sheets cannot readily collapse back to a graphitic structure. At the same time, some nanoflakes are like narrow belts or bent leaves, which may represent the parts that either has not been fully split apart or the parts that have restacked together due to capillary and the van der

Waals forces during the drying process. And what's more, mono- or bilayer graphene can also be seen in some of the TEM images. The various morphologies indicate that the combining reaction during the grind is not homogeneous.

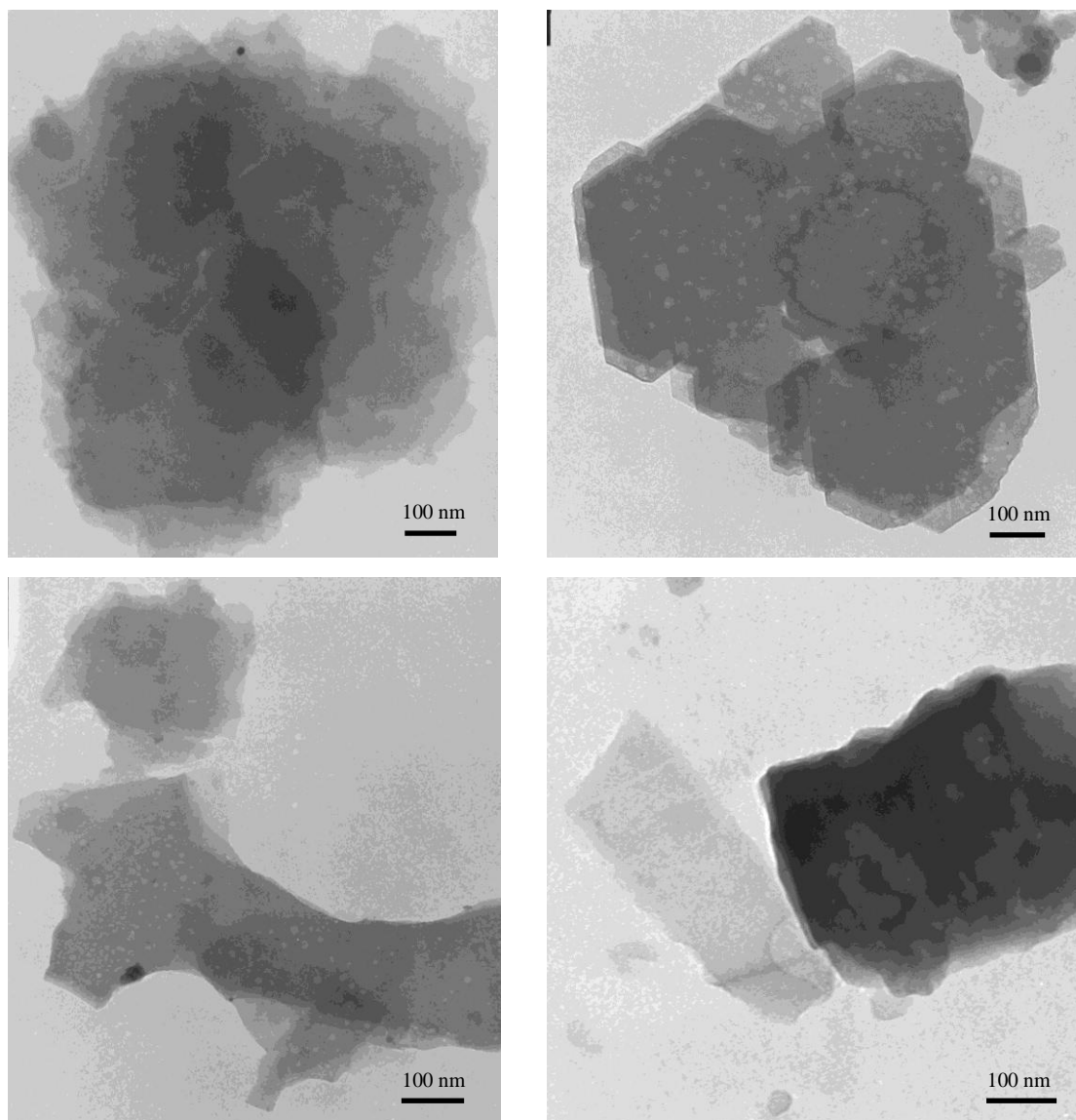


Figure 7. TEM images of carbon/IL composite (Instruct name: JEM-1200EX, 80.0 kV).

What we are interested here is the microstructure of the edge of the combined composite, which has close relationship with its electrochemical properties. So, though the information on the degree of graphene/graphite formation and on the number of layers, which can be yielded by Raman [26], can not be given here by SEM and TEM, it is enough to highlight the flake structures of graphene/OPFP with their edge plane characteristics.

Above experiments confirm the high exfoliation of graphite in the presence of OPFP during the grind. Based on this hypothesis, the attractive electroanalytical performance of the CILE can be understood easily. As has been reported, graphene, which displays excellent properties (such as large surface-to-volume ratio, high conductivity and electron mobility at room temperature, low energy dynamics of electrons with atomic thickness, robust mechanical and flexibility), has tremendous potential for electrochemical catalysis and biosensing as a novel electrode material [27]. Here it's reasonable to believe that the remarkable electron transfer kinetics, active electrocatalysis and sensitive sensing properties of CILE are mainly due to edge plane sites/defects that occur at the end of the graphene flakes [17, 19, 28-30].

4. CONCLUSIONS

The mechanical force produces mono- or multilayer graphene during the grinding process. And the OPFP molecules are prone to combine with the graphene, causing the avoidance of the agglomeration of the exfoliated flakes. The presence of graphene, which is edge plane characteristic, provides high density of electrochemical reactive sites on the surface of the paste electrode. Thus the CILE exhibits attractive electroanalytical performance for a wide range of analytes, notably improved sensitivity and increase of electron transfer rate. Relatively, the fabrication of this kind of functional electrode is simple than some other methods [23, 31, 32], thus it might be more popular in preparing some kinds of chemsensors and biosensors.

ACKNOWLEDGEMENTS

The authors gratefully acknowledge financial supports from the National Natural Science Foundation of China (Grant No. 21005086) and the Shandong Province Natural Science Foundation (No. ZR2011BQ029).

References

1. D. Wei, A. Ivaska, *Anal. Chim. Acta* 607 (2008) 126.
2. B. J. Privett, J. H. Shin, M. H. Schoenfish, *Anal. Chem.* 82 (2010) 4723.
3. N. Maleki, A. Safavi, F. Tajabadi, *Anal. Chem.* 78 (2006) 3820.
4. H. Liu, P. He, Z. Li, C. Sun, L. Shi, Y. Liu, G. Zhu, J. Li, *Electrochem. Commun.* 7 (2005) 1357.
5. Z. Zhu, L. Qu, Q. Niu, Y. Zeng, W. Sun, X. Huang, *Biosens. Bioelectron.* 26 (2011) 2119.
6. R.T. Kachoosangi, M.M. Musameh, I. Abu-Yousef, J.M. Yousef, S.M. Kanan, L. Xiao, S.G. Davies, A. Russell, R.G. Compton, *Anal. Chem.* 81 (2009) 435.
7. R. T. Kachoosangi; G. G. Wildgoose, R. G. Compton, *Electroanalysis* 19 (2007) 1483.
8. J. Ping, J. Wu, Y. Ying, *Electrochem. Commun.* 12 (2010) 1738.
9. M. M. Musameha, R. T. Kachoosangi, L. Xiao, A. Russell, R. G. Compton, *Biosens. Bioelectron.* 24 (2008) 87.
10. X. Zhang, Y. Cui, Z. Lv, M. Li, S. Ma, Z. Cui, Q. Kong, *Int. J. Electrochem. Sci.* 6 (2011) 6063.
11. R.L. David, *Handbook of Chemistry and Physics*; 87th ed., CRC Press, Boca Raton, 2006.
12. R.L. McCreery, *Chem. Rev.* 108 (2008) 2646.

13. C. Guo, Z. Lu, Y. Lei, C. Li, *Electrochem. Commun.* 12 (2010) 1237.
14. Y. Zhu, S. Murali, W. Cai, X. Li, J. W. Suk, J. R. Potts, R. S. Ruoff, *Adv. Mater.* 22 (2010) 3906.
15. K. S. Novoselov, A. K. Geim, S. V. Morozov, D. Jiang, Y. Zhang, S.V. Dubonos, I.V. Grigorieva, A.A. Firsov, *Science* 306 (2004) 666.
16. A. Safavi, N. Maleki, H. Ershadifar, F. Tajabadi, *Anal. Chim. Acta* 674 (2010) 176.
17. K. R. Ratinac, W. Yang, J. J. Gooding, P. Thordarson, F. Braet, *Electroanalysis* 23 (2011) 803.
18. C. Knieke, A. Berger, M. Voigt, R. N. K. Taylor, J. Röhr, W. Peukert, *Carbon* 48 (2010) 3196.
19. M. Tunckol, J. Durand, P. Serp, *Carbon* 50 (2012) 4303.
20. Y. Hernandez, V. Nicolosi, M. Lotya, F. M. Blighe, Z. Sun, S.a De, I. T. McGovern, B. Holland, M. Byrne, Y. K. Gun'Ko, J. J. Boland, P. Niraj, G. Duesberg, S. Krishnamurthy, R. Goodhue, J. Hutchison, V. Scardaci, A. C. Ferrari, J. N. Coleman, *Nat. Nanotechnol.* 3 (2008) 563.
21. C. Richard, F. Balavoine, P. Schultz, T. W. Ebbesen, C. Mioskowski, *Science* 300 (2003) 775.
22. D. Wang, D. Choi, J. Li, Z. Yang, Z. Nie, R. Kou, D. Hu, C. Wang, L. V. Saraf, J. Zhang, I. A. Aksay, J. Liu, *ACS Nano.* 3 (2009) 907.
23. K. Liu, J. Zhang, G. Yang, C. Wang, J. Zhu, *Electrochem. Commun.* 12 (2010) 402.
24. J. Penga, C. Hou, X. Liu, H. Li, X. Hu, *Talanta* 86 (2011) 227.
25. A. S. Patole, S. P. Patole, H. Kang, J.-B. Yoo, T.-H. Kim, J.-H. Ahn, *J. Colloid Interf. Sci.* 350 (2010) 530.
26. F. M. Koehler, A. Jacobsen, T. Ihn, K. Ensslin, W. J. Stark, *Nanoscale* 4 (2012) 3781.
27. T. Gan, S. Hu, *Microchim. Acta* 175 (2011)1.
28. C. E. Banks, T. J. Davies, G. G. Wildgoose, R. G. Compton, *Chem. Comm.* (2005) 829.
29. N. G. Shang, P. Papakonstantinou, M. McMullan, M. Chu, A. Stamboulis, A. Potenza, S. S. Dhesi, H. Marchetto, *Adv. Funct. Mater* 18 (2008) 3506.
30. D. W. Kimmel, G. LeBlanc, M. E. Meschievitz, D. E. Cliffel, *Anal. Chem.* 84 (2012) 685.
31. Y. Jiang, Q. Zhanga, F. Li, L. Niu, *Sensor. Actuat. B* 161 (2012) 728.
32. S. Hu, H. Zhu, S. Liu, J. Xiang, W. Sun, L. Zhang, *Microchim. Acta* 178 (2012) 211.